Available online at www.sciencedirect.com
SCIENCE DIRECT®
Journal of volcanology and geothermal research
ELSEVIER
Journal of Volcanology and Geothermal Research 131 (2004) 93–108
www.elsevier.com/locate/jvolgeores

Dynamics of magma ascent and fragmentation in trachytic versus rhyolitic eruptions

Margherita Polacci [a,*], Paolo Papale [a], Dario Del Seppia [a,b], Daniele Giordano [c,d], Claudia Romano [d]

[a] *Istituto Nazionale di Geofisica e Vulcanologia, sede di Pisa, Via della Faggiola 32, I-56126 Pisa, Italy*
[b] *Dipartimento di Scienze della Terra, Università di Pisa, Pisa, Italy*
[c] *Department of Earth and Environmental Sciences, University of Munich, Munich, Germany*
[d] *Dipartimento di Scienze Geologiche, Università Roma Tre, Rome, Italy*

Received 17 March 2003; accepted 26 September 2003

Abstract

We have performed a parametric study on the dynamics of trachytic (alkaline) versus rhyolitic (calc-alkaline) eruptions by employing a steady, isothermal, multiphase non-equilibrium model of conduit flow and fragmentation. The employed compositions correspond to a typical rhyolite and to trachytic liquids from Phlegrean Fields eruptions, for which detailed viscosity measurements have been performed. The investigated conditions include conduit diameters in the range 30–90 m and total water contents from 2 to 6 wt%, corresponding to mass flow rates in the range 10^6–10^8 kg/s. The numerical results show that rhyolites fragment deep in the conduit and at a gas volume fraction ranging from 0.64 to 0.76, while for trachytes fragmentation is found to occur at much shallower levels and higher vesicularities (0.81–0.85). An unexpected result is that low-viscosity trachytes can be associated with lower mass flow rates with respect to more viscous rhyolites. This is due to the non-linear combined effects of viscosity and water solubility affecting the whole eruption dynamics. The lower viscosity of trachytes, together with higher water solubility, results in delayed fragmentation, or in a longer bubbly flow region within the conduit where viscous forces are dominant. Therefore, the total dissipation due to viscous forces can be higher for the less viscous trachytic magma, depending on the specific conditions and trachytic composition employed. The fragmentation conditions determined through the simulations agree with measured vesicularities in natural pumice clasts of both magma compositions. In fact, vesicularities average 0.80 in pumice from alkaline eruptions at Phlegrean Fields, while they tend to be lower in most calc-alkaline pumices. The results of numerical simulations suggest that higher vesicularities in alkaline products are related to delayed fragmentation of magmas with this composition. Despite large differences in the distribution of flow variables which occur in the deep conduit region and at fragmentation, the flow dynamics of rhyolites and trachytes in the upper conduit and at the vent can be very similar, at equal conduit size and total water content. This is consistent with similar phenomenologies of eruptions associated with the two magma types.

Keywords: trachytic magma; conduit flow; eruption dynamics; numerical simulations

* Corresponding author. Tel.: +39-050-8311932; Fax: +39-050-8311942.
E-mail address: polacci@pi.ingv.it (M. Polacci).

0377-0273/03/$ – see front matter © 2003 Elsevier B.V. All rights reserved.
doi:10.1016/S0377-0273(03)00319-6

1. Introduction

Many explosive eruptions throughout the world involve the discharge into the atmosphere of magma belonging to calc-alkaline compositional suites. Volcanoes characterized by these magma compositions are mostly distributed around the Pacific basin, forming what is called the Circum-Pacific Fire Ring. Volcanic products from calc-alkaline magmas are characterized by glass compositions typically from dacitic to rhyolitic, crystal contents from nearly absent to more than 50 wt%, and total water contents from a few to several (7–8) wt% with respect to the crystal-free magma. Typical mass flow rates during sustained explosive phases of the eruptions range from $< 10^6$ to 10^9 kg/s (Cas and Wright, 1987; Sigurdsson et al., 2000). A variety of eruptive phenomena can occur during these phases, including formation of buoyant or Plinian to sub-Plinian eruptive columns often accompanied by partial collapses from their margins, generation and development of pyroclastic flows, up to partial or total collapse of the volcano edifice and caldera formation (Cioni et al., 2000; Wilson and Houghton, 2000; Pinel and Jaupart, 2003).

Besides calc-alkaline volcanoes, other explosive volcanoes discharge magma belonging to alkaline compositional suites with typical compositions from phonolite to trachyte. Although relevant properties like viscosity and volatile solubility of chemically evolved alkaline magmas can be significantly different from those of evolved calc-alkaline magmas (Carroll and Blank, 1997; Hess and Dingwell, 1996; Dingwell et al., 1998; Giordano et al., 2003; Romano et al., 2003), the general phenomenology of explosive phonolitic or trachytic eruptions is similar to that characterizing calc-alkaline eruptions.

During the last 20 years the methods of physical and mathematical modeling have evolved in volcanology as a very effective mean for the investigation of the complex non-linear dynamics characterizing volcanic processes, and as a tool for the prediction of volcanic scenarios and forecast of volcanic hazard (Dobran, 2001). Recent reviews of numerical models and applications in volcanology can be found in Gilbert and Sparks (1998) and Freundt and Rosi (1998). Most of these applications are focused on magmas with andesitic to rhyolitic compositions (Carey and Sigurdsson, 1985; Dobran, 1992; Papale and Dobran, 1994; Papale et al., 1998; Neri et al., 1998; Papale and Polacci, 1999; Melnik and Sparks, 1999; Polacci et al., 2001; Clarke et al., 2002), with a notable exception represented by the phonolitic eruptions of Vesuvius (Dobran, 1992; Papale and Dobran, 1993; Dobran et al., 1994; Ongaro et al., 2002; Todesco et al., 2002; Neri et al., 2003).

The aim of this paper is to provide a systematic comparative study of the dynamics of magma ascent and fragmentation for eruptions involving rhyolitic (calc-alkaline) and trachytic (alkaline) magmas. Due to their peculiar water solubility and viscosity patterns, trachytic magmas are found to result in distinct flow variable distributions within the conduit and different conditions at fragmentation, and in larger expected (and measured) pumice vesicularities with respect to rhyolitic magmas. However, the flow conditions at the volcanic vent are found to be similar, according to the same general phenomenology shown by explosive eruptions involving the two magma types.

2. Materials and methods

We have performed a parametric study where numerical simulations of the steady, isothermal, multiphase non-equilibrium dynamics of magma conduit flow and acceleration, fragmentation, and choking, are repeated by only changing the liquid composition (rhyolite or trachyte) in the input data.

The physics and mathematics of the employed magma ascent modeling are described in detail in previous works (Papale, 1999a, 2001). The model solves the mass and momentum balance equations for the gas and liquid (or liquid plus crystal) phases, which are allowed to move at different speeds. The homogeneous flow region at undersaturated volatile conditions, bubbly flow region below magma fragmentation, and gas particle flow region above fragmentation are all accounted

Table 1
Compositions of the liquid phase (wt%) employed in the simulations

Composition	SiO_2	TiO_2	Al_2O_3	Fe_2O_3	FeO	MnO	MgO	CaO	Na_2O	K_2O
Rhyolite	72.49	0.24	14.06	0.90	0.77	0.07	0.72	2.06	4.21	3.26
AMS trachyte	61.26	0.38	18.38	1.17	2.33	0.14	0.74	2.97	4.58	8.04
CI trachyte	60.74	0.27	19.22	1.12	2.25	0.18	0.28	2.11	5.28	6.32

Rhyolitic composition from Innocenti et al. (1982). AMS and CI compositions measured via electron microprobe (accelerating voltage 15 kV, spot size 20 μm, 10 nA beam current) on pumice samples from the B1 fallout layer (for AMS, Romano et al., in press) and V3 basal fallout layer at Voscone (for CI, Giordano et al., in review). Fe^{3+}/Fe^{2+} equal to 0.5 (Middlemost, 1989).

for. Mass balance equations account for gain (gas phase) or loss (liquid phase) of mass due to volatile exsolution, which is assumed to follow thermodynamic equilibrium. The momentum balance equations consider the change in momentum of each phase as due to pressure, gravity, inter-phase drag, wall friction, volatile exsolution, and (for the particles above fragmentation) particle–particle interaction forces. Complex sets of constitutive equations from the multiphase flow literature are employed for the different flow regimes. Magma fragmentation is assumed to occur when the stress due to elongation of magma upon acceleration along the conduit causes a rheological brittle response of magma (Maxwell, 1867), according to its viscoelastic nature (Webb and Dingwell, 1990). The two-point boundary value problem represented by steady flow of magma along the volcanic conduit is solved numerically along a non-homogeneous one-dimensional grid, with up-flow (conduit base) boundary conditions represented by magma composition and pressure, and down-flow (conduit exit) boundary conditions represented by either choking of the multiphase magmatic mixture, or atmospheric pressure. The specific down-flow boundary condition is not selected a-priori, but is itself part of the solution.

The employed compositions (reported in Table 1) are a typical rhyolite, also employed in previous numerical modeling studies (Papale et al., 1998; Papale and Polacci, 1999; Papale, 1999a, 2001), and a trachytic composition from Phlegrean Fields corresponding to that of the 4400 BP Agnano Monte Spina (AMS) (de Vita et al., 1999; Romano et al., 2003). In order to cover a wide range of possible conditions, water contents in the range 2–6 wt% and conduit diameters from 30 to 90 m have been employed in the parametric study. In addition, one subset of the simulations (conduit diameter 60 m, water content 2–6 wt%) has been repeated using the trachytic liquid composition of the 37 ka Campanian Ignimbrite (CI) eruption (Signorelli et al., 1999, 2001; Giordano et al., 2003). This was done to test if small differences in trachytic liquid compositions, and associated different magmatic properties, can translate into distinct distributions of the flow variables along the volcanic conduit. Magma temperature is fixed at 1100 K in order to focus on the effects of different compositions. This temperature is within the typical range of both magma types (Sigurdsson, 2000). In order to keep the numerical runs to a minimum, crystal content, conduit length, and stagnation pressure have been kept constant, and water has been employed as the only volatile component. Table 2 reports the input data of the performed simulations. For further simplicity, only particles of one size (diameter 0.2 mm) and density (corresponding to the density of the homogeneous liquid+crystal phase) are assumed to flow in the gas particle region above magma fragmentation.

Table 2
Input data for the performed simulations

Conduit length (km)	5
Stagnation pressure (MPa)	122.5
Temperature (K)	1100
Conduit diameter (m)	30–90
Total water content (wt%)	2–6
Particle size (mm)	0.200
Composition	Rhyolite–Trachyte (AMS, CI)
Crystal content (vol%)	0

3. Magma properties

The different rhyolitic and trachytic compositions correspond to different magma properties, which in turn determine different ascent dynamics. The magma properties viscosity, density, and water solubility, which appear in the transport equations, are examined below.

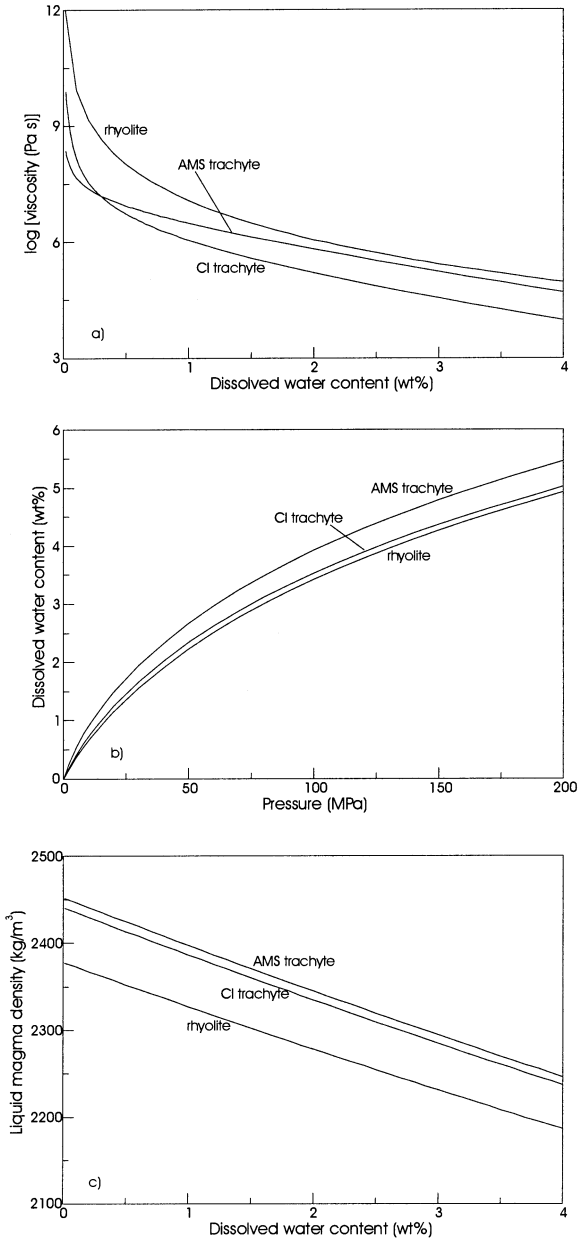

Fig. 1. Calculated (a) liquid viscosity, (b) water solubility and (c) liquid density for the employed trachytic and rhyolitic magma compositions. The employed models are described in the text.

Fig. 1a shows the liquid viscosity of the employed rhyolitic and trachytic compositions at the constant temperature of 1100 K employed in the simulations. Rhyolitic viscosity is calculated according to Hess and Dingwell (1996), while AMS and CI trachytic viscosities are calculated according to Romano et al. (2003) and Giordano et al. (2003). All the viscosity models are based on the Vogel–Fulcher–Tamman semi-empirical equation (Vogel, 1921; Fulcher, 1925; Tammann and Hesse, 1926) for the viscosity of glass-forming liquids, modified to take into explicit account the amount of dissolved water. These equations have six parameters that have been distinctly calculated for typical rhyolitic compositions and for the AMS and CI trachytes.

As it emerges from Fig. 1a, the dry viscosity of rhyolite at 1100 K is more than three orders of magnitude larger than that of AMS trachyte at the same temperature. However, the AMS trachyte displays a smaller initial viscosity drop with increasing amounts of water, nearly leveling off the viscosity difference at dissolved water contents of 1.5–2 wt%. Differently, the viscosity of the CI trachyte is significantly higher than that of the AMS trachyte at dry conditions, but significantly lower (up to nearly one order of magnitude) for water contents larger than only 0.5 wt%.

It is worth noting that due to the high potential of water loss from the experimental samples at high temperature and/or high water contents, viscosity determinations of hydrous samples (on which the model calculations in Fig. 1a rest) were done at temperatures close to the glass transition, and for water contents less than 4 wt%, while high-T measurements were only done on dry samples (Hess and Dingwell, 1996; Giordano et al., 2003; Romano et al., 2003). This implies an uncertainty in the viscosity curves in Fig. 1a, requiring the development and standardization of new techniques for measuring high-T hydrous viscosities in silicate melts.

Fig. 1b shows water solubility for the employed rhyolitic and trachytic compositions. Water solu-

bility is determined by the model in Papale (1997), which allows to take into account the liquid composition in terms of the 10 major oxides reported in Table 1, and pressures well above 100 MPa at which non-Henrian behavior is important (Papale, 1999b). The figure shows that the solubility of water in the AMS trachyte is significantly larger than that in rhyolite. The difference amounts to 10% at 200 MPa, 15% at 100 MPa, 20% at 50 MPa, and 40% at 10 MPa. Water solubility in the CI liquid is still higher than that in rhyolite, but not as much as for the AMS trachyte. Considering a total water content of 4 wt% (with respect to the crystal-free magma), the saturation pressure corresponds to 104, 126, and 132 MPa for the AMS trachyte, CI trachyte, and rhyolite, respectively.

Fig. 1c shows the liquid density for the employed rhyolitic and trachytic compositions, calculated according to Lange and Carmichael (1987) and Lange (1994). The density of the trachytic liquid is 2–3% larger than that of rhyolite. In both cases the dissolution of 5 wt% H_20 in the liquid determines a density decrease of about 10%.

In case a different temperature in the range 900–1300 K is used, no significant differences in the trends reported in Fig. 1 emerge. Therefore, qualitative changes in the simulation results presented below are not expected if a different temperature is employed in the simulations, as long as the same temperature is assumed for all magma types.

4. Results

For simplicity, the results presented in this section pertain to the simulations made with rhyolitic and AMS trachytic compositions. The simulations pertaining to CI trachyte are described in less detail and are introduced in the discussion, in order to emphasize some of the conclusions of the present work and highlight the complex, non-linear role played by magma properties in the conduit flow dynamics.

According with the aim of the paper, the following description of results, as well as the discussion, are focused on the comparison between the conduit dynamics as obtained with the different rhyolitic and trachytic magma compositions. The roles of different water contents and conduit diameters at constant magma composition are not examined. These roles have been described elsewhere for dacitic to rhyolitic calc-alkaline compositions (Papale et al., 1998). The present results show qualitatively similar patterns, which are therefore not examined here.

A summary of calculated fragmentation and exit conditions for the investigated rhyolitic and AMS trachytic compositions, along with the exsolution and fragmentation depths and mass flow rates, are reported in Table 3. All the performed simulations correspond to the achievement of choked flow conditions at the conduit exit, implying an exit pressure greater than (or in the limit equal to) atmospheric. Exceptions are simulations AMS-2-30 and rh-2-30, for which the small conduit diameter and low water content employed result in a very large pressure drop along the conduit, and the atmospheric pressure turns out to be larger than the back pressure required for flow choking. Therefore, the down-flow boundary (conduit exit) condition for these two simulations corresponds to magmatic pressure equal to atmospheric, and the flow is not choked.

Figs. 2, 3 and 5 show the distribution of flow variables along the conduit for the performed simulations. In these figures, plots labeled a, b, and c refer to constant conduit diameters and water contents of 2, 4, and 6 wt%. The overall flow variable distributions are remarkably different for rhyolites and trachytes in the deep conduit region below magma fragmentation, while differences reduce very much above fragmentation up to the conduit exit.

Fig. 2 shows the calculated non-dimensional pressure distribution along the conduit, and it includes, for comparison, the curve corresponding to lithostatic pressure (calculated assuming a constant rock density of 2500 kg/m^3 required to produce a lithostatic pressure equal to the stagnation pressure of magma at the magma chamber level). All other conditions being equal, the pressure gradient in the deep conduit region is larger (in module) for rhyolitic than for trachytic magma com-

Table 3
Summary of calculated conditions for the performed simulations

Run		Fragmentation conditions				Exit conditions					
	z_{exs} (m a.c.e.)	z (m a.c.e.)	α	P (MPa)	v_p (m/s)	α	P (MPa)	v_g (m/s)	v_p (m/s)	ρ_{mix} (kg/m^3)	$\dot{m}$ (kg/s$\times 10^{-7}$)
AMS-2-30	2384	2750	0.8377	2.91	3.50	0.9951	0.10	139.1	115.0	12.2	0.10
AMS-4-30	646.9	2271	0.8120	8.68	16.3	0.9836	0.71	213.1	181.9	41.8	0.54
AMS-6-30	<0	1786	0.8342	11.8	25.4	0.9807	1.30	241.3	212.4	49.8	0.75
AMS-2-60	2799	3244	0.8245	3.76	8.11	0.9895	0.20	173.7	134.1	26.2	1.00
AMS-4-60	743.7	3046	0.8212	8.49	28.1	0.9722	1.24	197.9	177.0	70.6	3.55
AMS-6-60	<0	2724	0.8456	11.2	41.7	0.9695	2.12	225.3	205.9	78.8	4.61
AMS-2-90	3067	3588	0.8215	3.97	12.5	0.9833	0.33	166.0	132.7	41.6	3.53
AMS-4-90	777.4	3496	0.8284	8.23	37.8	0.9629	1.70	186.7	171.9	94.2	10.3
AMS-6-90	<0	3295	0.8521	10.8	55.2	0.9613	2.69	225.2	206.5	99.8	13.2
CI-2-60	2971.5	3652.2	0.7899	4.97	14.69	0.9767	0.50	157.3	130.9	58	2.15
CI-4-60	<0	3634.1	0.8277	8.44	16.25	0.9597	1.84	188.9	171.2	102	4.97
CI-6-60	<0	3519.6	0.8596	10.5	25.36	0.9606	2.76	229	209.2	101	6.02
rh-2-30	1685	2012	0.6689	5.73	1.63	0.9952	0.10	128.2	109.8	11.8	0.09
rh-4-30	<0	1249	0.6906	15.2	11.1	0.9811	0.80	206.4	177.8	46.6	0.59
rh-6-30	<0	741	0.7389	19.6	20.0	0.9759	1.62	235.0	210.7	60.5	0.91
rh-2-60	2011	2388	0.6466	8.41	4.23	0.9892	0.20	175.2	135.7	26.3	1.01
rh-4-60	<0	2011	0.7019	15.0	18.8	0.9689	1.36	197.6	175.7	76.8	3.83
rh-6-60	<0	1515	0.7564	18.5	30.1	0.9656	2.38	225.6	207.5	86.4	5.09
rh-2-90	2296	2746	0.6417	8.85	6.70	0.9825	0.34	166.9	134.5	42.6	3.66
rh-4-90	<0	2499	0.7089	14.7	25.3	0.9584	1.86	190.3	171.8	103	11.3
rh-6-90	<0	2079	0.7648	17.9	38.8	0.9569	3.01	222.5	206.6	108	14.3

α, P, v, $\dot{m}$, z and ρ stay for the gas volume fraction, pressure, velocity, mass flow rate, vertical coordinate and density. Subscripts *exs*, *g*, *p* and *mix* stay for exsolution level, gas phase, particles and gas+liquid (+crystals) mixture. a.c.e means above conduit entrance. In the first column AMS and CI stay for trachyte, rh stays for rhyolite, and the first and second number refer to the total water content and conduit diameter of each simulation.

position. Accordingly, the magmatic pressure in this region is significantly lower for rhyolites than for trachytes. For example, referring to the cases with 4 wt% water, 1 km above the conduit entrance the magmatic pressure for rhyolites is from 2.5 to 20 MPa lower than that of trachytes, this difference increasing with decreasing conduit diameter. Accordingly, in the range of considered conditions the magmatic pressure is always less than lithostatic for rhyolites, while in the deep conduit regions it can be larger than lithostatic for trachytes, particularly for large conduit diameters and water contents.

In all the performed simulations, the magmatic pressure at fragmentation is much less than lithostatic. The maximum difference between lithostatic and magmatic pressure (corresponding to the fragmentation level) is much larger for rhyolites (45–85 MPa) than for trachytes (26–68 MPa). Conversely, the fragmentation pressure is larger for rhyolites, ranging from 6 to 20 MPa, than for trachytes, from 3 to 12 MPa (Table 3). As anticipated, the pressure distribution after fragmentation, as well as the distribution of any other flow variable, is very similar for both magma types when the same conduit diameter and total water content are considered.

Fig. 3 shows the calculated gas volume fraction distribution along the volcanic conduit. Two relevant results arise from the comparison between the two considered magma compositions. Firstly, all other conditions being equal, the gas volume fraction at the conduit entrance is always larger for rhyolites than for trachytes, as a result of larger water solubility for the latter magma type (Fig. 1b). Secondly, fragmentation of rhyolites occurs much deeper in the conduit than for trachytes (this is also visible in Fig. 2), and at a

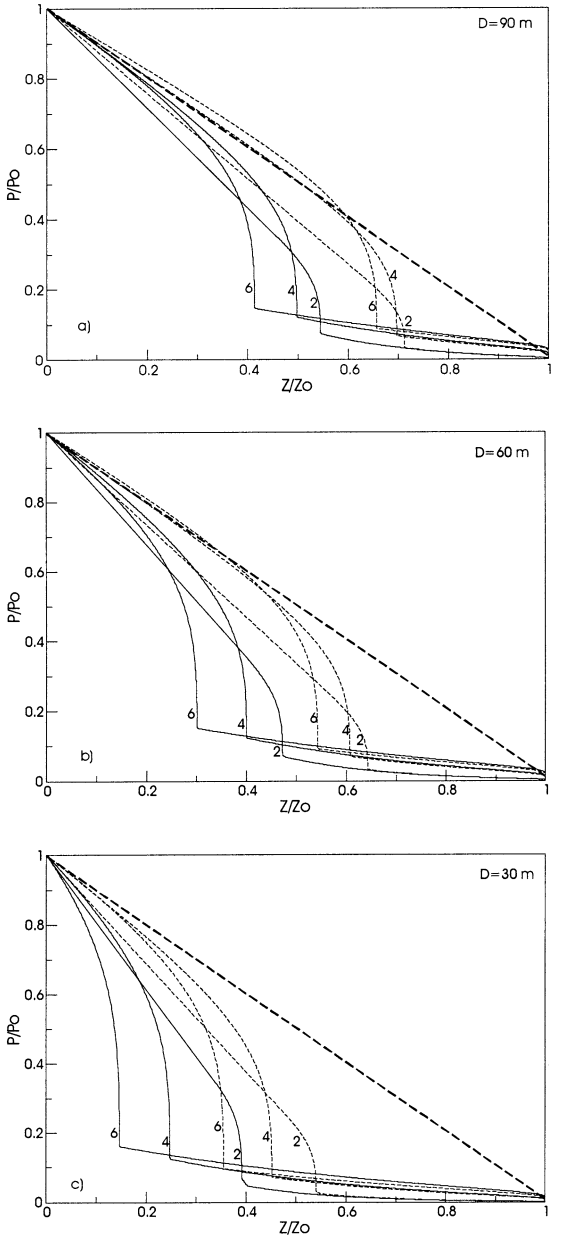

Fig. 2. Calculated non-dimensional pressure distributions along the conduit. This figure, as Figs. 3–7, refers to simulations corresponding to AMS trachyte (dashed lines) and rhyolite (thin lines) in Table 3. The numbers 2, 4 and 6 next to the curves indicate the corresponding total water content in weight percent. The bold dashed line indicates lithostatic pressure.

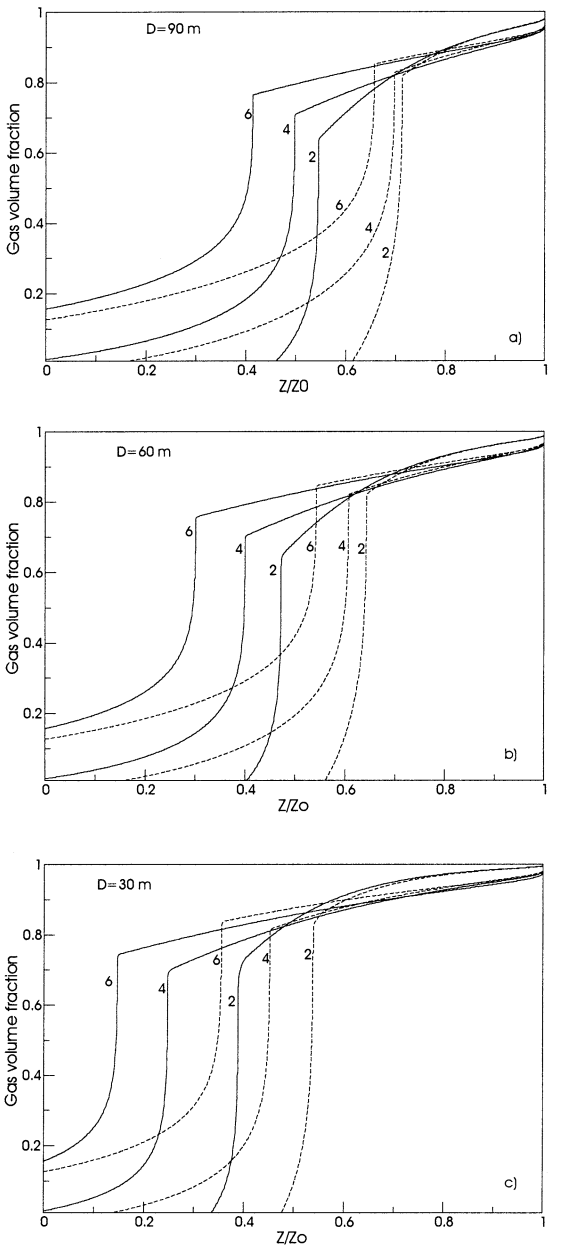

Fig. 3. Calculated gas volume fraction distributions along the conduit for the simulations in Table 3.

significantly lower gas volume fraction. The fragmentation conditions are shown in Fig. 4 in terms of magma vesicularity (a) and depth (b). In the range of considered conditions, fragmentation of rhyolitic magma occurs at a vesicularity in the

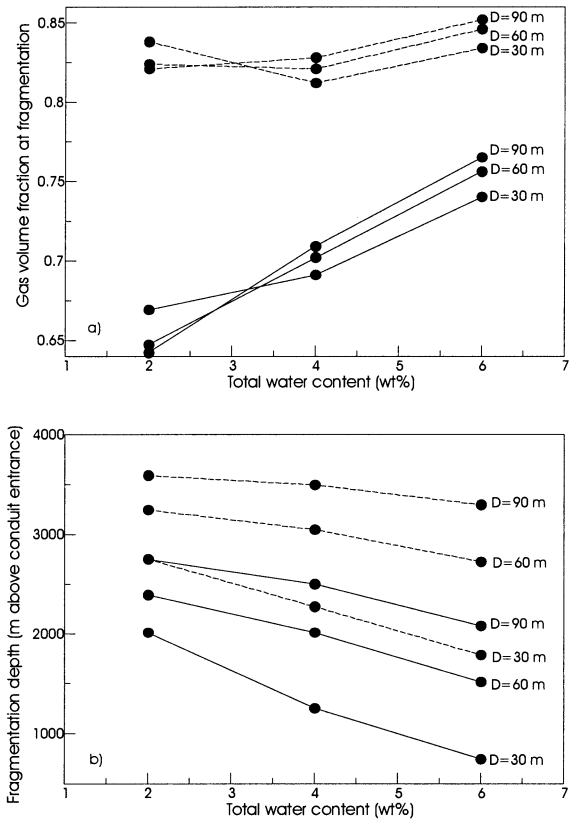

Fig. 4. Calculated fragmentation conditions in terms of (a) magma vesicularity and (b) fragmentation depth, for the simulations in Table 3.

range 0.64–0.76, and that of trachytes in the range 0.81–0.85 (Fig. 4a and Table 3). No clear trend of magma vesicularity at fragmentation with total water content emerges for trachytes, while for rhyolites the fragmentation vesicularity is found to increase with increasing water content. For both magma types, conduit diameter variations from 30 to 90 m do not produce important changes in the vesicularity at fragmentation.

Fragmentation depths (height above conduit base) vary from 1780 to 3590 m for trachytes, and from 740 to 2750 m for rhyolites (Fig. 4b and Table 3). For both magma types, clear trends of increasing fragmentation depth with increasing water content and decreasing conduit diameter are found. All other conditions being equal, the fragmentation depth for trachytes is 750–1200 m shallower than for rhyolites. Table 3 also shows that as for fragmentation, the water exsolution level (assumed to occur at water saturation in the present calculations) is 650–800 m deeper for rhyolites than for trachytes (for water contents of

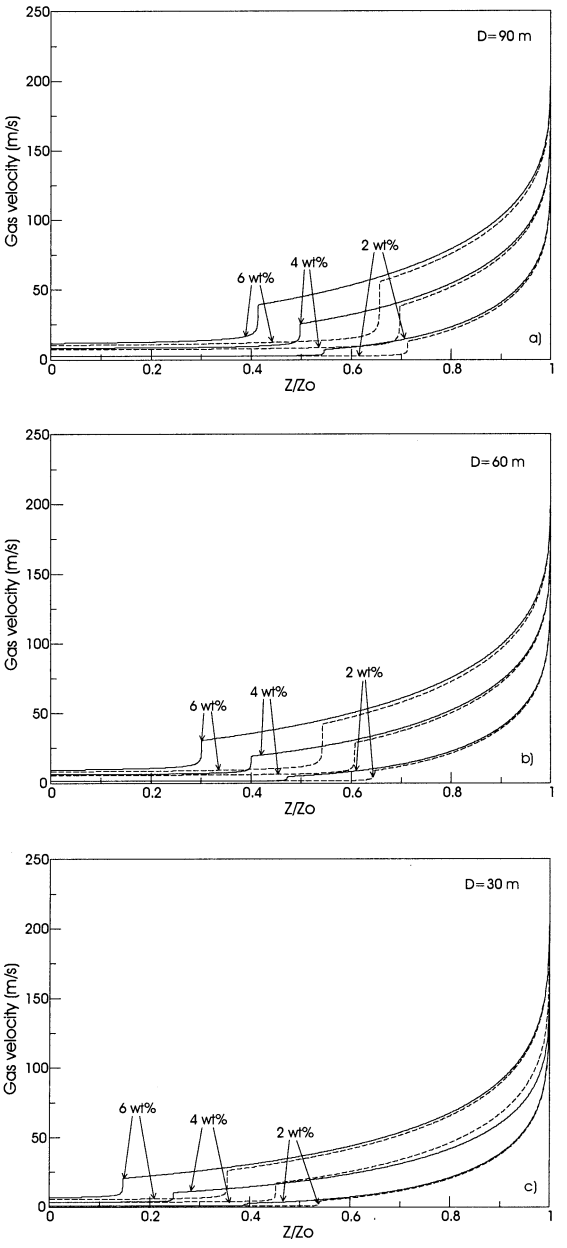

Fig. 5. Calculated gas velocity distributions along the conduit for the simulations in Table 3.

6 wt%, volatile exsolution occurs within the magma chamber for both magma types).

The distribution of gas velocity along the conduit is shown in Fig. 5. Here the particle velocity distribution is not shown since it is indistinguishable from that of the gas phase, except very close to the conduit exit where differences of up to 40 m/s are found (Table 3). The velocity distributions for the two magma types are very similar both before and after magma fragmentation, differences occurring only close to the fragmentation level. All other conditions being equal, fragmentation velocities are larger for trachytes than for rhyolites. Fragmentation velocities are in the range 3.5–56 m/s for trachytes, and 1.6–40 m/s for rhyolites, increasing with increasing total water content and conduit diameter (Table 3).

Fig. 6 shows the calculated (a) mass flow rates and (b–f) vent conditions as a function of water content for all the performed simulations in Table 3. Compared with the different flow variable distributions along the conduit (Figs. 2, 3 and 5), and different fragmentation conditions (Fig. 4), rhyolites and trachytes show a remarkably similar behavior at the conduit exit. For most variables reported in Fig. 6, the points corresponding to trachytes and rhyolites are nearly coincident for water contents of 2 wt%. A maximum difference of 20% is found in the exit pressure for the two magma types at a total water content of 6 wt% and conduit diameter of 30 m, with the exit pressure for trachyte being lower than that for rhyolite (Fig. 6e). In the range of considered conditions, mass flow rates cover two orders of magnitude from 10^6 to 10^8 kg/s, and are very similar for the two magma types (Fig. 6a). Rhyolites are characterized by slightly larger mass flow rates, except for the lowest conduit diameter and water content employed, where the relationships are reversed. Differences in mass flow rates vary from 8–21% at 6 wt% water, to 1–10% at 2 wt% water (Fig. 6a and Table 3).

In the range of considered conditions, exit gas volume fractions vary from 0.957 to 0.995, exit gas velocities from 128 to 241 m/s, exit particle velocities from 110 to 212 m/s, exit pressures from 0.1 (atmospheric) to 3 MPa, and exit mixture densities from 12 to 108 kg/m^3.

5. Discussion

5.1. Flow variable distributions along the volcanic conduit

The most note worth results of the preceding section can be summarized as follows. The distribution of flow variables in the deep conduit region below fragmentation, the flow conditions at fragmentation, and the position of the fragmentation level are remarkably different for rhyolite and AMS trachyte as a consequence of the different properties of the two magma types; yet, the two employed liquid compositions do not result in large differences of mass flow rates and of the flow variables at shallow conduit levels approaching the volcanic conduit exit.

It is important to remark here that the performed simulations do not take into account all the effects that might be associated with different liquid compositions. As an example, it is implicitly assumed that the kinetic delay to volatile exsolution does not play a different role in the employed rhyolitic and trachytic liquids. In addition, limiting the investigation to the case where only fine, non-vesicular ash is produced by magma fragmentation, we effectively assume that the mechanics of magma fragmentation acts in the same way for the two magma types. In fact, if different proportions of pumice and ash, or different vesicle textures in pumice, are produced by different mechanical behavior of the stressed liquids or by different fragmentation conditions, then the flow conditions in the shallow conduit region and the flow variable distributions at the conduit exit would not be the same anymore (Papale, 2001). The present investigation is therefore limited to the analysis of the effects related to the different magma properties viscosity, water solubility, and density, reported in Fig. 1. However, despite this simplification, the results of this work are not intuitive and require a deep inspection in order to be understood. In the following we will discuss the various roles of the above magma properties in determining the different flow variable distributions described above.

The calculated water solubility for the AMS trachyte is significantly larger than that for rhyo-

lite (Fig. 1b). This implies that more water is dissolved in the trachytic liquid, and, accordingly, a lower volume is occupied by the gas phase, at any given pressure below saturation. Along with the viscosity curves in Fig. 1a, this implies that the viscosity of the AMS trachyte is lower than that of the rhyolite at any given pressure (see also Eqs. 54 and 55 in Papale, 2001). At the conduit entrance, where the pressure is the same for the two magma types, the mixture viscosity of the

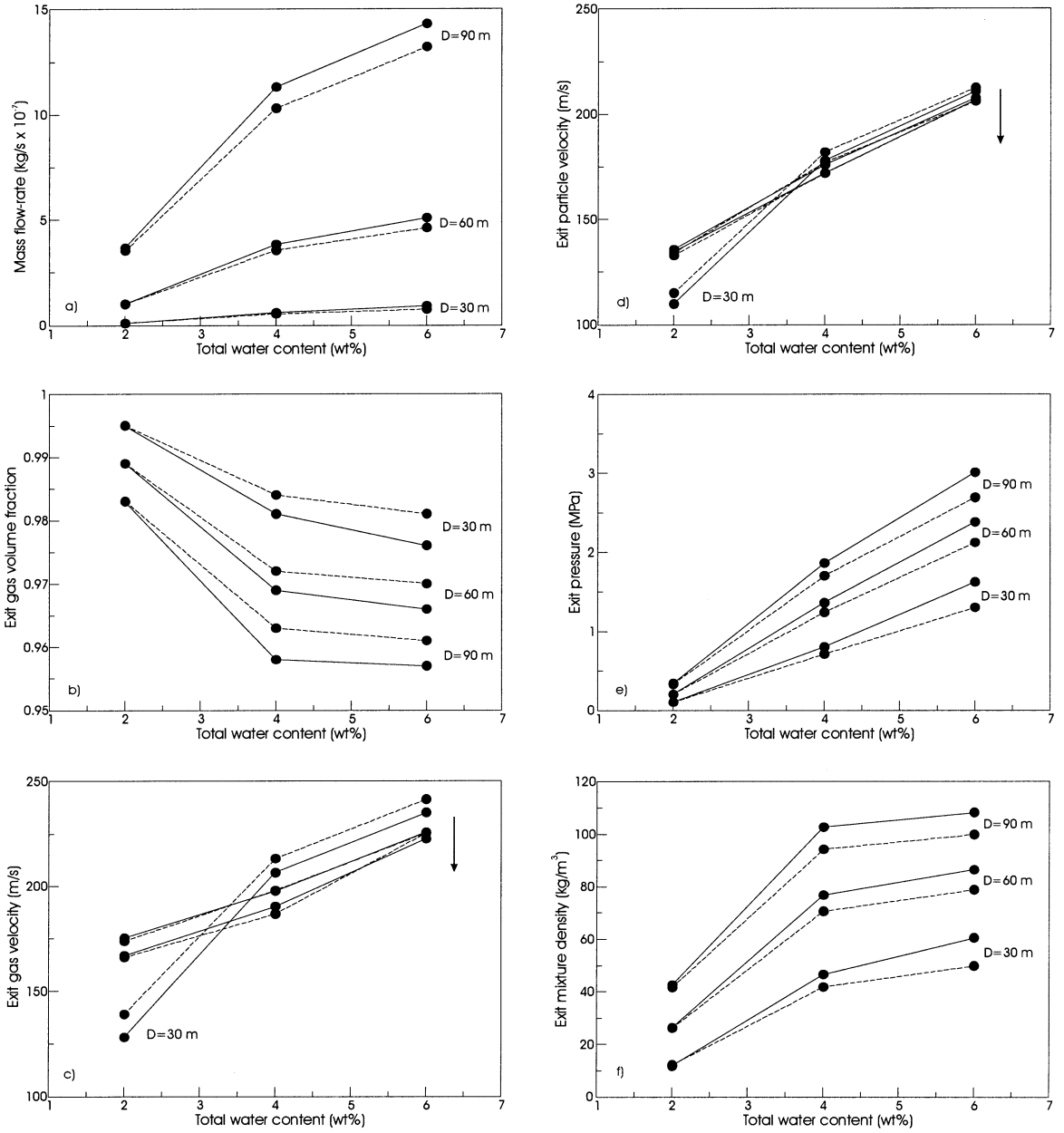

Fig. 6. Calculated (a) mass flow rates, and (b–f) conduit exit conditions for the simulations in Table 3. The arrow in (c) and (d) goes in the direction of increasing conduit diameter.

AMS trachyte is from 3/5 to 3/10 that characterizing rhyolite (Fig. 7).

Pressure and viscosity concur to a feedback effect whereby small viscosity differences are amplified to produce largely different distributions of the flow variables below the fragmentation level. Magma fragmentation is preceded by a region where a rapid breakdown of flow conditions occurs as a consequence of this feedback effect. Higher viscosity results in larger (in magnitude) pressure gradients in the deep conduit regions, and accordingly, in larger gradients of any other flow quantity including velocity.

In the present case, larger viscosity in rhyolite is associated with lower water solubility. Therefore, all other input data (apart from liquid composition) being equal, at a given height below fragmentation the rhyolitic magma is characterized by lower pressure, larger gas volume fraction and mixture viscosity, and larger gradients of pressure (in magnitude) and gas volume fraction (Figs. 2, 3 and 7). Magma velocity results from the mass flow rate of the eruption, which in turn is a complex function of the flow variable distribution along the conduit and of the height of the fragmentation level, as discussed in the following. The performed simulations show that the mass flow rate for the AMS trachyte turns out to be slightly lower than for rhyolite (all other input to the flow model being equal). Together with lower liquid density (Fig. 1c) and gas volume fraction distributions of rhyolite as outlined above, the above results in velocities and velocity gradients (or elongational strain rates) in the conduit region below fragmentation which are larger for the rhyolitic than for the trachytic magma (Fig. 5).

Fragmentation of magma occurs when magma viscosity times the vertical gradient of velocity overcomes a critical value, independently from the specific fragmentation criterion adopted, either the strain rate (Papale, 1999a, and this work) or gas bubble overpressure criterion (Melnik, 2001). The above picture and the described feedback effect imply therefore that fragmentation conditions are achieved deeper in the conduit for the rhyolitic magma (Figs. 2–5 and Table 3). The less viscous trachytic magma needs to be more stretched in order to fragment, implying further depressurization, expansion, and acceleration. Accordingly, fragmentation velocity, vesicularity, and strain rate are larger, while pressure is lower, for the trachytic than for the rhyolitic magma (Table 3).

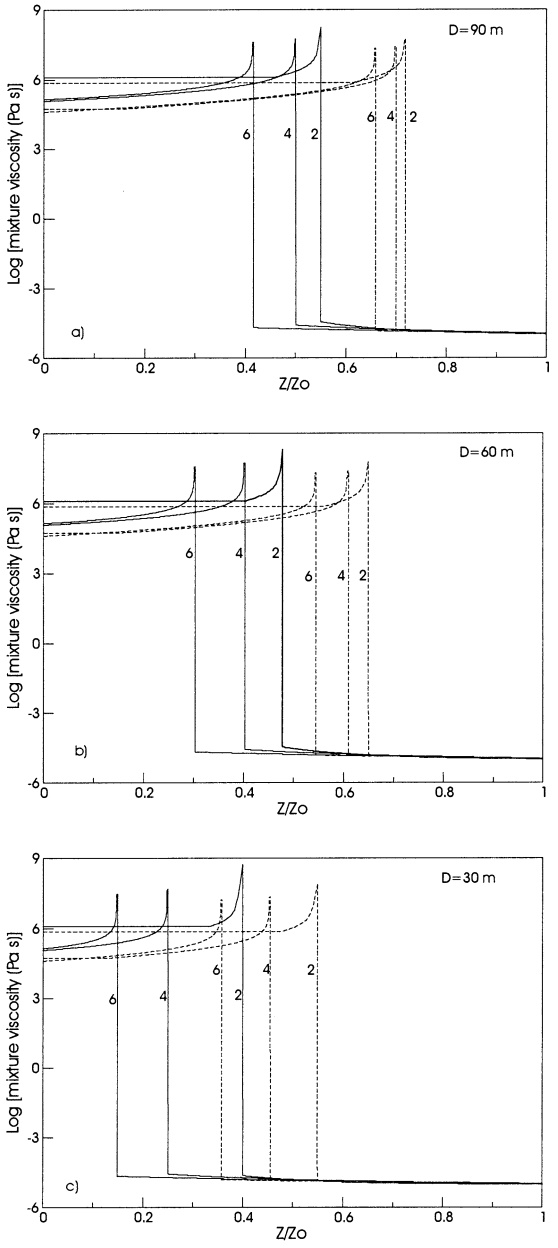

Fig. 7. Calculated mixture viscosity distributions along the conduit for the simulations in Table 3.

5.2. Mass flow rates

Although Fig. 6a shows relatively simple trends of mass flow rates with compositions, the present investigation leads to conclude that quite complex relationships exist between the composition of the erupted magma and the mass flow rate realized. These complex relationships are examined in the following.

Magma viscosity is known to be a crucial quantity in determining the mass flow rate, as a consequence of its dissipative effect on the mechanical energy of the flowing fluid. A progressive decrease of viscosity accompanying a compositional change from rhyolite to dacite has been found to result in a mass flow rate increase up to a factor of 5 (Papale et al., 1998). Conversely, in the present case the less viscous AMS trachyte is associated with a lower, instead of higher, mass flow rate (Fig. 6a). In order to understand this apparent inconsistency, it is necessary to take into account the distribution of magma viscosity along the volcanic conduit reported in Fig. 7.

While magma viscosity is very high below fragmentation (up to 10^8–10^9 Pa s in the present simulations), above that level the viscosity of the two-phase gas particle mixture drops by several orders of magnitude, approaching that of the continuous gas phase (about 10^{-5} Pa s). The dissipative action of viscous forces is therefore concentrated in the highly viscous bubbly flow region below fragmentation. Total dissipation by viscous forces, which affects the capability of magma to flow, or the mass flow rate of the eruption, is therefore a combination of magma viscosity and length of the bubbly flow region, or height of the fragmentation level. The AMS trachytic magma is characterized by lower viscosity (working towards larger mass flow rate) and higher fragmentation level (working towards lower mass flow rate). The calculations show that the two effects nearly cancel each other, with a slight dominance of fragmentation height over absolute viscosity, resulting in a similar but lower mass flow rate for the trachytic magma (Fig. 6a).

The larger viscosity and lower water solubility of rhyolite shown in Fig. 1a,b result therefore in larger mass flow rates. Once again, it is worth noting that if, on one hand, a larger viscosity implies larger resistance to flow, it also favors a more rapid achievement of fragmentation conditions, forcing pressure to decrease more rapidly in the conduit. Therefore, on the other hand, a larger viscosity works to a certain extent towards increased mass flow rate, decreasing the length of the highly viscous (and highly dissipative) bubbly flow region. A similar conclusion also holds for water solubility. A less amount of dissolved water at a given pressure implies larger viscosity (lower mass flow rate), favoring a more rapid achievement of fragmentation conditions (larger mass flow rate). The general conclusion arising from the above observations is that even the direction to which the eruptive dynamics can move in response to changes of magma composition cannot be simply predicted, without accounting for the above non-linear relationships (or without performing apposite numerical simulations).

An example that illustrates the above, and which is useful for further investigating the dynamics of trachytic as compared to rhyolitic eruptions, is given by the simulations pertaining to the CI trachytic composition. In this case, water solubility is still larger than that of rhyolite, but not as much as for the AMS trachyte (Fig. 1b), mainly as a consequence of a less amount of calcium and potassium oxides (Table 1). On the contrary, the viscosity of CI is the least among the three magma types considered (Fig. 1a). According to the discussion above, an a priori prediction of whether the mass flow rate associated with the CI trachyte will be larger or lower than that of the AMS trachyte and rhyolite in Fig. 6a would be very challenging.

Table 3 and Fig. 8 report the results of the additional simulations involving the CI trachyte. In this case, magma fragmentation is reached at levels even shallower than for the AMS magma, although at about the same magma vesicularity (0.80–0.86) (Fig. 8a). Mixture viscosity in the bubbly flow region exhibits the lowest values, but this high viscosity region is the longest (Fig. 8b). The numerical simulations show that the net result is highest mass flow rates (Fig. 8c), suggesting that the effect of lower magma viscosity is, in this case, dominant over that of longer bubbly flow region.

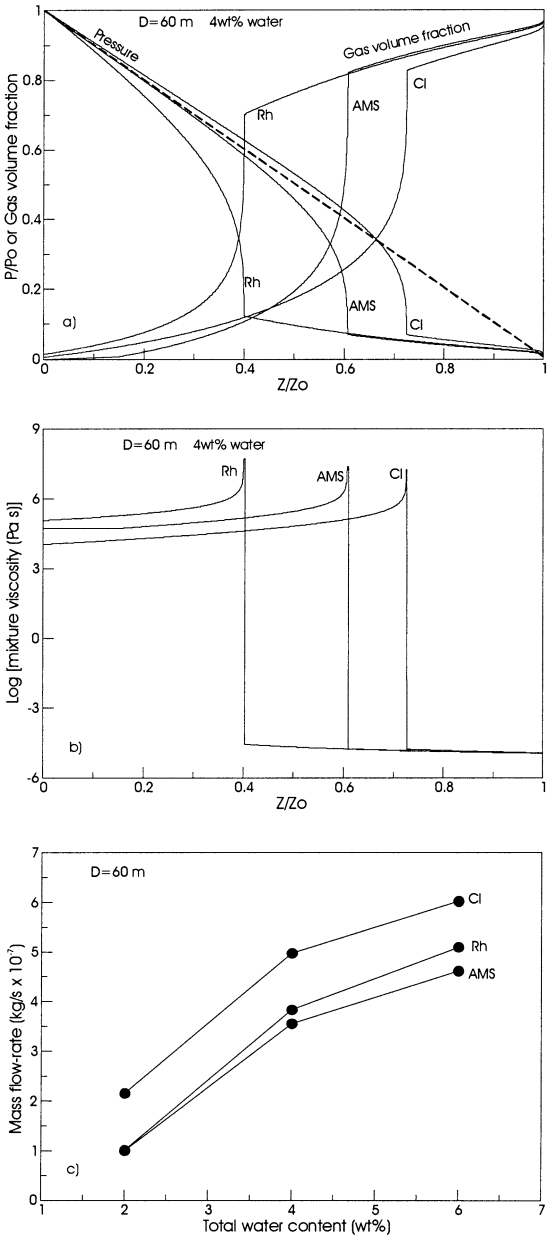

Fig. 8. Flow variable distributions along the conduit and mass flow rates for the simulations done by employing the CI trachyte composition in Table 1. The curves corresponding to rhyolitic and AMS trachytic compositions (also in Table 1) are reported for comparison. (a) Non-dimensional pressure and gas volume fraction; (b) mixture viscosity; (c) mass flow rate. Simulation conditions correspond to a fixed conduit diameter of 60 m in all plots, and to 4 wt% total water content in (a), (b), and 2–6 wt% total water in (c). The bold dashed line in (a) indicates lithostatic pressure.

Additionally, the flow variable distributions in the upper conduit region and at the conduit exit are appreciably different from those of the AMS trachyte and rhyolite (Fig. 6a, Table 3). This suggests that the similar flow conditions in the shallow conduit region for the simulations pertaining to the AMS trachyte and rhyolite descend, as for the similar mass flow rates, from a balance of counteracting effects produced by the peculiar magma property distributions in Fig. 1.

Comparison of simulation results in Table 3 offers many other examples, not discussed here, of the non-linear relationships between magma composition (or properties) and magma ascent dynamics.

5.3. Comparison with natural pumice

Specific fragmentation conditions in terms of gas volume fraction (or magma vesicularity) can be tested through comparison with natural pumice products of rhyolitic and trachytic compositions, as crystal and vesicle textures have proved to preserve information related to magmatic processes occurring in volcanic conduits (Klug and Cashman, 1996; Polacci et al., 2001; Klug et al., 2002). In particular, textures in pumice clasts that do not show evidence of post-fragmentation expansion can be assumed to be representative of the state of magma at fragmentation (Polacci et al., 2001). Therefore, measured clast vesicularities can be directly compared with calculated gas volume fractions at fragmentation. Textural investigation has mostly focused on juvenile material of andesitic to rhyolitic composition, and limited data are available for pyroclasts discharged by eruptions of alkaline compositional suites. Recent characterization of trachytic pumice clasts from eruptions at Phlegrean Fields (Polacci et al., 2003) has shown that average vesicularities in the so-called ‘microvesicular’ pumice type, which is considered representative of the bulk volume of the discharged magma (Polacci et al., 2001, 2003; Rosi et al., 2003), is close to 0.80. Similar values are reported for alkaline phonolites from Vesuvius (Gurioli et al., 2003). These average vesicularities are larger than average values commonly found in calc-alkaline dacitic or rhyolitic pumice,

typically around 0.75 (Gardner et al., 1996). Since microvesicular pumices do not present evidence of post-fragmentation expansion, they are assumed to preserve the original magma vesicularity and can be directly compared to calculated vesicularities. The present simulation results provide an explanation of the generally higher vesicularities found in alkaline pumice. According to the above discussion, the high fragmentation vesicularity in trachytic pumice is the result of low viscosity and large water solubility of this type of magma. Within the relatively wide range of conditions considered in the present work, calculated fragmentation vesicularities in trachytes vary from 0.81 to 0.85, while they range from 0.64 to 0.76 for rhyolite, consistent with observations on pumice textures.

Calculated fragmentation vesicularities in trachyte also show a rather small range of values compared to rhyolite. In order to evaluate this result and check it with observations, additional textural measurements on trachytic pumice clasts, as well as additional numerical simulations of trachytic magma flow in a wide range of conditions (e.g. varying conduit length and magma temperature, and considering other volatile species besides water), need to be accomplished.

6. Conclusions

The present parametric study represents a first, fundamental step towards the quantification of volcanic processes for volcanoes characterized by the discharge of magma with trachytic compositions. Phlegrean Fields represent the best and most well-known example of these volcanoes. Here, hundreds of thousands of people live within a big caldera formed as a consequence of giant eruptions which produced Plinian columns and extremely destructive and long-traveling pyroclastic flows, often with a significant contribution of external water in enhancing explosivity (Di Vito et al., 1999). This extremely risky situation translates into the need of an assessment of volcanic hazard, and quantification of possible volcanic scenarios.

The present work attempts to compare the simulated trachytic magma ascent dynamics with that, much more investigated in the past, related to rhyolitic magmas. This comparison reveals systematic differences in the distributions of flow variables within the conduit. Mass flow rates and conduit exit conditions are affected in a complex, strongly non-linear way, so that the net effect of different magma compositions on conduit ascent dynamics is unpredictable without the aid of numerical simulations.

In addition, this study shows once again how large and complex the effects of different magma properties on the dynamics of volcanic eruptions can be. It is implicit that uncertainties in the characterization of basic magma properties like viscosity and water solubility should be reduced to a minimum, especially if we are interested in testing numerical models with real eruption data. Unfortunately, at present a true comparison is still limited by many factors including availability of sin-eruptive data (practically non-existent at Phlegrean Fields and in general for trachytic volcanoes), limited knowledge of magmatic properties over the whole range of physical and chemical conditions of volcanic interest, and limited capability of available numerical models to account for a large spectrum of volcanic processes.

Acknowledgements

We wish to thank GNV for supporting this work through research project n 2000/02-17, and O. Melnik and J. Gardner for their helpful reviews.

References

Carey, S., Sigurdsson, H., 1985. The May 18, 1980 eruption of Mount St. Helens 2. Modeling of the dynamics of the Plinian phase. J. Geophys. Res. 90, 2948–2958.

Carroll, M., Blank, J., 1997. The solubility of water in phonolitic melts. Am. Mineral. 82, 549–556.

Cas, R.A.F., Wright, J., 1987. Volcanic Successions – Modern and Ancient, Chapman and Hall, New York.

Cioni, R., Marianelli, P., Santacroce, R., Sbrana, A., 2000. Plinian and Subplinian eruptions. In: Sigurdsson, H., Houghton, B.F., McNutt, S.R., Rymer, H., Stix, J. (Eds.), Encyclopedia of Volcanoes. Academic press, San Diego, CA, pp. 477–494.

Clarke, A.B., Voight, B., Neri, A., Macedonio, G., 2002. Transient dynamics of vulcanian explosions and column collapse. Nature 415, 897–901.

de Vita, S., Orsi, G., Civetta, A., Carandente, A., D'Antonio, M., Deino, A., di Cesare, T., Di Vito, M.A., Fisher, R.V., Isaia, R., Marotta, E., Necco, A., Ort, M., Pappalardo, L., Piochi, M., Southon, J., 1999. The Agnano Monte Spina eruption (4100 years BP) in the restless Campi Flegrei caldera (Italy). J. Volcanol. Geotherm. Res. 91, 269–301.

Dingwell, D.B., Hess, K.U., Romano, C., 1998. Viscosity data for hydrous peraluminous granitic melts; comparison with a metaluminous model. Am. Mineral. 83, 236–239.

Di Vito, M.A., Isaia, R., Orsi, G., Southon, J., de Vita, S., D'Antonio, M., Pappalardo, L., Piochi, M., 1999. Volcanism and deformation since 12000 years at the Campi Flegrei caldera (Italy). J. Volcanol. Geotherm. Res. 91, 221–246.

Dobran, F., 1992. Non-equilibrium flow in volcanic conduits and applications to the eruptions of Mt. St. Helens on May 18, 1980, and Vesuvius in AD 79. J. Volcanol. Geotherm. Res. 49, 285–311.

Dobran, F., 2001. Volcanic Processes: Mechanisms in Material Transport. Kluwer Academic, New York.

Dobran, F., Neri, A., Todesco, M., 1994. Assessing pyroclastic flow hazard at Vesuvius. Nature 367, 551–554.

Freundt, A., Rosi, M., 1998. From Magma to Tephra. Springer, Berlin.

Fulcher, G.S., 1925. Analysis of recent measurements of the viscosity of glasses. Am. Ceram. Soc. J. 8, 339–355.

Gardner, J.E., Thomas, R.M.E., Jaupart, C., Tait, S.R., 1996. Fragmentation of magma during Plinian volcanic eruptions. Bull. Volcanol. 58, 144–162.

Gilbert, J.S., Sparks, R.S.J., 1998. The Physics of Explosive Volcanic Eruptions. The Geological Society, London.

Giordano, D., Romano, C., Papale, P., Dingwell, D.B., 2003. Viscosity of trachytes from Phlegrean Fields, and comparison with basaltic, phonolitic, and rhyolitic melts. J. Volcanol. Geotherm. Res., in review.

Gurioli, L., Houghton, B., Cashman, K., Cioni, R., 2003. Complex changes in eruption dynamics and the transition between Plinian and phreatomagmatic activity during the 79 AD eruption of Vesuvius. Bull. Volcanol., in review.

Hess, K.-U., Dingwell, D.B., 1996. Viscosities of hydrous leucogranitic melts: A non-Arrhenian model. Am. Mineral. 81, 1297–1300.

Innocenti, F., Manetti, P., Mazzuoli, R., Pasquarè, G., Villari, L., 1982. Anatolia and North-western Iran. In: Thorpe, R.S. (Ed.), Andesites. Wiley and Sons, New York, pp. 327–349.

Klug, C., Cashman, K.V., 1996. Permeability development in vesiculating magmas: implications for fragmentations. Bull. Volcanol. 58, 87–101.

Klug, C., Cashman, K.V., Bacon, C.R., 2002. Structure and physical characteristics of pumice from the climactic eruption of Mt Mazama (Crater Lake), Oregon. Bull. Volcanol. 64, 486–501.

Lange, R.A., 1994. The effects of H_2O, CO_2 and F on the density and viscosity of silicate melts. Mineral. Soc. Am. Rev. Mineral. 30, 331–369.

Lange, R.A., Carmichael, I.S.E., 1987. Densities of Na_2O–K_2O–CaO–MgO–FeO–Fe_2O_3–Al_2O_3–TiO_2–SiO_2 liquids: new measurements and derived partial molar properties. Geochim. Cosmochim. Acta 53, 2195–2204.

Maxwell, J.C., 1867. On the dynamical theory of gases. Phil. Trans. R. Soc. London 157, 49–88.

Melnik, O., 2001. Dynamics of two-phase conduit flow of high viscosity gas-saturated magma: large variations of sustained explosive eruptions intensity. Bull. Volcanol. 62, 153–170.

Melnik, O., Sparks, R.S.J., 1999. Nonlinear dynamics of lava dome extrusion. Nature 40, 37–41.

Middlemost, E.A.K., 1989. Iron oxidation ratios, norms and the classification of volcanic rocks. Chem. Geol. 77, 19–26.

Neri, A., Papale, P., Macedonio, G., 1998. The role of magma composition and water content in esplosive eruptions: II. Pyroclastic dispersion dynamics. J. Volcanol. Geotherm. Res. 87, 95–115.

Neri, A., Papale, P., Del Seppia, D., Santacroce, R., 2003. Couplet conduit and atmospheric dispersal dynamics of the AD 79 Plinian eruption of Vesuvius. J. Volcanol. Geotherm. Res. 120, 141–160.

Ongaro, T., Neri, A., Todesco, M., Macedonio, G., 2002. Pyroclastic flow hazard assessment at Vesuvius (Italy) by using numerical modeling. II. Analysis of flow variables. Bull. Volcanol. 64, 178–191.

Papale, P., 1997. Thermodynamic modelling of the solubility of H_2O and CO_2 in silicate liquids. Contrib. Mineral. Petrol. 126, 237–251.

Papale, P., 1999a. Strain-induced magma fragmentation in explosive eruptions. Nature 397, 425–428.

Papale, P., 1999b. Modeling of the solubility of a two-component H_2O+CO_2 fluid in silicate liquids. Am. Mineral. 84, 477–492.

Papale, P., 2001. The dynamics of magma flow in volcanic conduits with variable fragmentation efficiency and non-equilibrium pumice degassing. J. Geophys. Res. 106, 11043–11065.

Papale, P., Dobran, F., 1993. Modeling the ascent of magma during the Plinian eruption of Vesuvius in AD 79. J. Volcanol. Geotherm. Res. 58, 101–132.

Papale, P., Dobran, F., 1994. Magma flow along the volcanic conduit during the plinian and pyroclastic flow phases of the May 18, 1980, Mount St. Helens eruption. J. Geophys. Res. 99, 4355–4373.

Papale, P., Polacci, M., 1999. Role of carbon dioxide in the dynamics of magma ascent in explosive eruptions. Bull. Volcanol. 60, 583–594.

Papale, P., Neri, A., Macedonio, G., 1998. The role of magma composition and water contents in explosive eruptions. I. Conduit ascent dynamics. J. Volcanol. Geotherm. Res. 87, 75–93.

Pinel, V., Jaupart, C., 2003. Magma chamber behavior beneath a volcanic edifice. J. Geophys. Res. 102, DOI 10.1029/2002JB001751.

Polacci, M., Papale, P., Rosi, M., 2001. Textural heterogeneities in pumices from the climactic eruption of Mount Pina-

tubo, 15 June 1991, and implications for magma ascent dynamics. Bull. Volcanol. 63, 83–97.

Polacci, M., Pioli, L., Rosi, M., 2003. The Plinian phase of the Campanian Ignimbrite eruption (Phlegrean Fields, Italy): evidence from density measurements and textural characterization of pumice. Bull. Volcanol. 65, 418–432, DOI 10.1007/S00445-002-0268-4.

Romano, C., Giordano, D., Papale, P., Mincione, V., Hess, K.U., Dingwell, D.B., Rosi, M., 2003. The viscosities of hydrous melts from Vesuvius and Phlegrean Fields systems. Chem. Geol., in press.

Rosi, M., Landi, P., Polacci, M., Di Muro, A., Zandomeneghi, D., 2003. Role of conduit shear on ascent of the crystal-rich magma feeding the 800 yr BP Plinian eruption of Quilotoa Volcano (Ecuador). Bull. Volcanol., DOI 10.1007/S00445-003-0312-Z.

Signorelli, S., Vaggelli, G., Francalanci, L., Rosi, M., 1999. Origin of magmas feeding the Plinian phase of the Campanian Ignimbrite eruption, Phlegrean Fields Italy: constraints based on matrix-glass and glass-inclusion compositions. J. Volcanol. Geotherm. Res. 91, 199–220.

Signorelli, S., Vaggelli, G., Romano, C., Carroll, M.R., 2001. Volatile element zonation in Campanian Ignimbrite magmas (Phlegrean Fields, Italy): evidence from the study of glass inclusions and matrix glasses. Contrib. Mineral. Petrol. 140, 543–553.

Sigurdsson, H., 2000. Introduction. In: Sigurdsson, H., Houghton, B.F., McNutt, S.R., Rymer, H., Stix, J. (Eds.), Encyclopedia of Volcanoes. Academic press, San Diego, CA, pp. 1–13.

Sigurdsson, H., Houghton, B.F., McNutt, S.R., Rymer H., Stix J., 2000. Encyclopedia of Volcanoes. Academic press, San Diego, CA.

Tammann, G., Hesse, W., 1926. Die Abhängigkeit der Viskosität von der Temperatur bei unterkühlten Flüssigkeiten. Z. Anorg. Allg. Chem. 156, 245–257.

Todesco, M., Neri, A., Esposti Ongaro, T., Papale, P., Macedonio, G., Santacroce, R., Longo, A., 2002. Pyroclastic flow hazard assessment at Vesuvius (Italy) by using numerical modelling. Large-scale dynamics. Bull. Volcanol. 64, 155–177.

Vogel, D.H., 1921. Temperaturabhängigkeitsgesetz der Viskosität von Flüssigkeiten. Phys. Z. 22, 645–646.

Webb, S.L., Dingwell, D.B., 1990. Non-Newtonian rheology of igneous melts at high stresses and strain rates: experimental results for rhyolite, andesite, basalt and nephelinite. J. Geophys. Res. 95, 15695–15701.

Wilson, C.J.N., Houghton, B.F., 2000. Pyroclastic transport and deposition. In: Sigurdsson, H., Houghton, B.F., McNutt, S.R., Rymer, H., Stix, J. (Eds.), Encyclopedia of Volcanoes. Academic Press, San Diego, CA, pp. 545–554.